

Novel Cytotoxic Annonaceous Acetogenins from *Annona muricata*

Fang-Rong Chang and Yang-Chang Wu*

Graduate Institute of Natural Products, Kaohsiung Medical University, Kaohsiung 807, Taiwan, Republic of China

Received January 26, 2001

Seven new annonaceous acetogenins, muricins A–G (**1–7**), as well as five known compounds, a mixture of muricatetrocin A (**8**) and muricatetrocin B (**9**), longifolicin (**10**), corrossolin (**11**), and corrossolone (**12**), were isolated from the seeds of *Annona muricata*. The structures of all isolates were elucidated and characterized by spectral and chemical methods. These acetogenins showed significantly selective in vitro cytotoxicities toward the human hepatoma cell lines Hep G₂ and 2,2,15.

Many plants of the Annonaceae have been used in folk medicine and as insecticides. Among the constituents of these materials, annonaceous acetogenins, known to have potent anticancer and pesticidal activities, are now regarded as the major active principles. Annonaceous acetogenins, a rather new class of natural compounds isolated only from the Annonaceae, are usually C₃₅–C₃₇ fatty acid derivatives connecting a variable number of tetrahydrofuran (THF) or tetrahydropyran (THP) rings and a terminal lactone moiety. So far, more than 300 compounds, many of which are stereoisomers, have been found and published, and their biological activities, such as anticancer cytotoxic, antiparasitic, insecticide, and immunosuppressive effects, have been further explored and found to relate to ATP production.^{1–3}

Annona muricata L. (Annonaceae) is a well-known tropical fruit tree named “sour sop” or “guanabana”, which is mainly distributed in the Americas and in Southeast Asia. To date, there have been more than 40 annonaceous acetogenins isolated from the stems, leaves, and seeds of this plant.³ In the previous study of annonaceous acetogenins from *Annona muricata* by Li et al., three annonaceous acetogenins, muricatins A–C, were found from the extract of the stem bark.⁴ In our current investigation of the seeds of this species, seven new annonaceous acetogenins, muricins A–G (**1–7**), along with five known compounds, a mixture of muricatetrocin A (**8**) and muricatetrocin B (**9**),⁵ longifolicin (**10**),⁶ corrossolin (**11**),⁷ and corrossolone (**12**),⁷ were isolated and further purified by reversed-phase HPLC (see Figure 1). The structures of the new compounds described herein contain a monotetrahydrofuran ring with one or two neighboring hydroxyl groups. Among them, compounds **1** and **2** are stereoisomers, and their absolute configurations were determined through analyses of their Mosher ester derivatives.^{8,9} More importantly, compound **2** is the first example of an annonaceous acetogenin that possesses a hydroxyl group of the *S*-configuration substituted at C-4. The configuration of the hydroxyl group at C-4 is generally assigned as *R*.^{1–3} Moreover, compounds **4** and **5** are the first annonaceous acetogenins that possess a C₃₃ skeleton; the others are all C₃₅ or C₃₇ compounds. In in vitro cancer cell lines, all of the isolated compounds except **5** and **7** showed potent cytotoxicities, and some showed selective cytotoxicities against the human hepatoma cell lines Hep G₂ and 2,2,15.

Results and Discussion

Muricin A (**1**) was isolated as a white waxy solid, [α]_D²⁵ +7.2° (*c* 0.25, CHCl₃). The [M + Na]⁺ peak in the FABMS at *m/z* 619 suggested the molecular weight as 596, and the molecular formula of C₃₅H₆₅O₇ was confirmed by HRFABMS. The UV spectral absorption at 210 nm and the IR spectral absorption at 1740 cm⁻¹ indicated the presence of an α,β -unsaturated γ -lactone group, positive to Kedde's reagent. The successive EIMS peaks at *m/z* 578, 560, and 542 implied the presence of at least three hydroxyl groups. In the ¹H NMR spectrum, the signals at δ 7.18 (1H, H-33), 5.06 (1H, H-34), 3.81 (1H, H-4), 2.54 (1H, H-3a), 2.47 (1H, H-3b), and 1.41 (3H, H-35) verified the presence of an α,β -unsaturated γ -lactone with a hydroxyl group at the C-4 position (see Table 1). The signals at δ 3.81 (2H, H-15, 18) and 3.41 (1H, H-19), as well as the ¹³C NMR peaks at δ 81.8 (C-18), 79.3 (C-15), and 74.4 (C-19), indicated the presence of a mono-THF ring with one flanking hydroxyl in a *threo* conformation.¹⁰ A close examination of the ¹H NMR spectrum showed that the proton resonances for the two methylene groups of the mono-THF ring, which were observed at δ 1.97 (H-16a, 17a) and 1.62 (H-16b, 17b), corresponded to the *trans* conformation.¹¹ By making the (*R*)- and (*S*)-Mosher ester derivatives by Hoye's methodology,¹² the absolute configurations at C-4 and C-19 of compound **1** could be confirmed as *R* and *R*, respectively (see Table 2).

Two of the hydroxyl groups were suspected to be a vicinal diol due to the proton signal at δ 3.41 (2H) and the ¹³C NMR peaks at δ 74.9 and 74.2. By making the acetonide derivative, the downfield shifts of two protons from δ 3.41 to 3.60 for two of the three methylene protons on OH-bearing carbons and the chemical shift of six protons at δ 1.36 (2 × CH₃, *s*) in the ¹H NMR spectrum verified the presence of a vicinal diol group (see Table 3). The conformation of this vicinal diol was assigned as *threo* on the basis of a comparison of its NMR chemical shifts with literature data.¹³

The placements of the THF ring and the diol were established by close examination of the EIMS fragmentation of **1** (see Figure 2). The THF ring was placed between C-15 and C-18 on the basis of the EIMS fragments at *m/z* 351 and 281, and the vicinal diol was located at C-26/C-27 on the basis of the EIMS fragments at *m/z* ([711]→[621]→531→441) of the TMS derivative.

Finally, the absolute configuration at C-34 of **1** was determined by the CD method.¹⁴ A positive π - π^* Cotton effect ($\Delta\epsilon > 0$) clearly indicated that the stereochemistry

* To whom correspondence should be addressed. Tel: +886-7-3121101, ext. 2197. Fax: +886-7-3114773. E-mail: yachwu@cc.kmu.edu.tw.

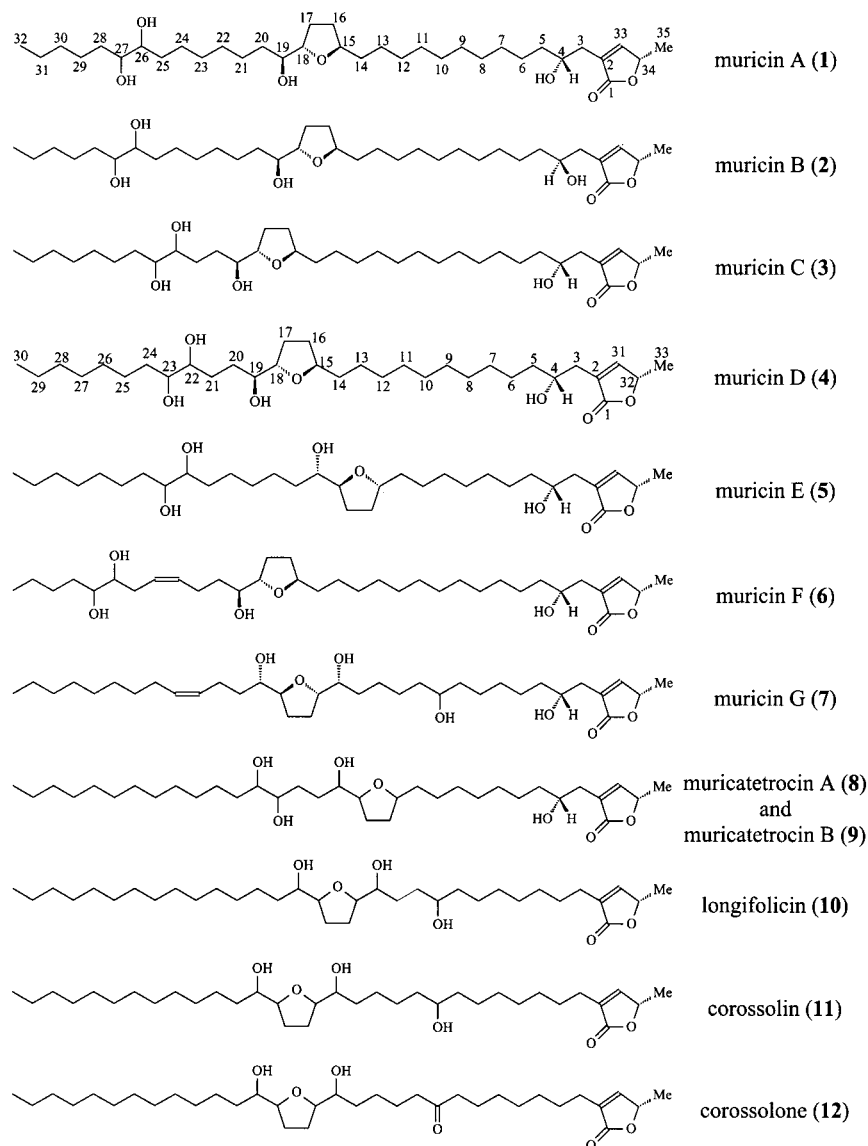


Figure 1. Seven new annonaceous acetogenins (**1–7**) and five known acetogenins (**8–12**) isolated from the seeds of *Annona muricata*.

at C-34 on the γ -lactone fragment should be of the (*S*)-configuration. Although we tried to determine the absolute stereochemistry of the carbinol centers at C-26/C-27 by Mosher methodology, the absolute stereochemistries at these positions remain undefined due to the indistinguishable chemical shifts of H-26 and H-27 in the ^1H NMR spectrum.

Muricin B (**2**) was isolated as a white waxy solid, $[\alpha]^{25}_{\text{D}} 0^\circ$ (*c* 0.11, CHCl_3). It was separated following compound **1** by reversed-phase HPLC with a solvent system of MeOH/ H_2O (88:12) in which **1** and **2** showed retention times at 13.7 and 14.2 min, respectively (Develosil ODS-5 column, 250×4.6 mm i.d., flow rate of 1 mL/min). The HRFABMS confirmed the molecular formula of $\text{C}_{35}\text{H}_{65}\text{O}_7$. The NMR spectral and MS data of compound **2** were very similar to those of compound **1**. Like compound **1**, the ^1H and ^{13}C NMR signals indicated the presence of an α,β -unsaturated γ -lactone with a hydroxyl group at the C-4 position and a mono-THF ring with one flanking hydroxyl group in a relative conformation of *trans*/*threo* according to the method of Fujimoto et al. (see Table 1).¹⁵ The normal-form tail of **2** was corroborated by the absorptions in the IR at 1740 cm^{-1} and the UV λ_{max} at 210 nm. A vicinal diol was confirmed by making its acetonide derivative, and its conformation was determined as *threo* on the basis of the comparison of

the ^1H and ^{13}C NMR data with compound **1**. The EIMS data, similarly to compound **1**, determined the placement of the THF ring and the diol at C-15/C-18 and C-26/C-27, respectively (see Figure 2). The positive $\pi-\pi^*$ Cotton effect ($\Delta\epsilon > 0$) of **2** in the CD spectrum indicated the stereochemistry at C-34 on the γ -lactone fragment to be of the (*S*)-configuration.

All of the NMR spectral and MS data indicated that compounds **1** and **2** are stereoisomers. For determining the absolute stereochemistries, their Mosher ester derivatives were prepared and compared (see Table 2). The only difference between **1** and **2** is the stereochemistry at C-4. The minor, but clear difference between the (*S*)- and (*R*)-MTPA esters permitted us to conclude that the configurations of C-4 and C-19 of **2** are *S* and *R*, while the configurations of C-4 and -19 of **1** are *R* and *R*. This is the first report of an annonaceous acetogenin with the *S*-configuration of the hydroxyl group at C-4. In addition, both compounds **1** and **2** are also the first examples of annonaceous acetogenins in which the THF ring is initialized at C-15. Although the absolute stereochemistries of the 1,2-diol in **1** and **2** remain unsolved (the MTPA data for the critical protons could not be differentiated), these two compounds suggest that orientations of the terminal lactone ring and a hydroxyl group at C-4 can alter bioactivities

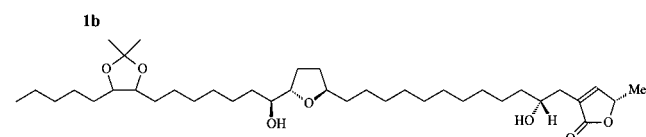
Table 1. ^1H and ^{13}C NMR Chemical Shifts of Compounds **1** and **2**

	muricin A		muricin B	
	δ (^1H)	δ (^{13}C)	δ (^1H)	δ (^{13}C)
1		174.9		174.6
2		131.2		131.9
3a	2.54 (m)	32.2	2.53 (m)	32.4
3b	2.47 (m)		2.49 (m)	
4	3.81 (m)	69.8	3.79 (m)	69.8
5	1.2–1.5	37.1	1.2–1.5	37.2
6–13	1.2–1.5	25.3–29.8	1.2–1.5	25.5–30.4
14	1.2–1.5	35.3	1.2–1.5	35.4
15	3.81 (m)	79.3	3.79 (m)	79.3
16	1.97, 1.62 (m)	25.3–29.8	1.98, 1.63 (m)	25.5–30.4
17	1.97, 1.62 (m)	25.3–29.8	1.98, 1.63 (m)	25.5–30.4
18	3.81 (m)	81.8	3.79 (m)	81.8
19	3.41 (m)	74.4	3.40 (m)	74.5
20	1.5–1.6	33.1–33.3	1.5–1.6	33.3–33.7
21–24	1.2–1.5	25.3–29.8	1.2–1.5	25.5–30.4
25	1.2–1.5	33.1–33.3	1.2–1.5	33.3–33.7
26	3.41 (m)	74.9 ^a	3.40 (m)	74.7 ^a
27	3.41 (m)	74.2 ^a	3.40 (m)	74.3 ^a
28	1.2–1.5	33.1–33.3	1.2–1.5	33.3–33.7
29	1.2–1.5	25.3–29.8	1.2–1.5	25.5–30.4
30	1.2–1.5	31.8	1.2–1.5	31.9
31	1.2–1.5	22.5	1.2–1.5	22.7
32	0.86 (t, $J = 6.7$)	13.9	0.87 (t, $J = 6.7$)	14.1
33	7.18 (d, $J = 1.6$)	152.1	7.18 (d, $J = 1.2$)	151.9
34	5.06 (qd, $J = 6.8, 1.6$)	78.0	5.06 (qd, $J = 6.4, 1.2$)	78.0
35	1.41 (d, $J = 6.8$)	18.9	1.41 (d, $J = 6.8$)	19.1

^a Assignments may be interchangeable.

Table 2. ^1H NMR Data of the (*S*)- and (*R*)-Mosher Esters of **1** and **2**

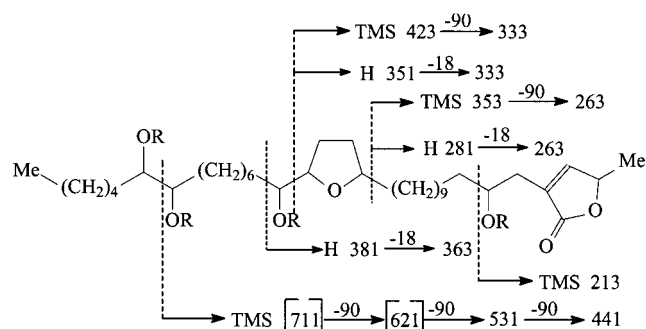
proton	1				2			
	S-MTPA	R-MTPA	$\Delta\delta_{S-R}$	config	S-MTPA	R-MTPA	$\Delta\delta_{S-R}$	config
H-3a	2.67	2.68	-0.01		2.63	2.53	+0.01	
H-3b	2.58	2.59	-0.01		2.57	2.40	+0.17	
H-33	6.96	6.96	0		6.72	6.65	+0.07	
H-34	4.89	4.90	-0.01	4 <i>R</i>	5.09	5.05	+0.04	4 <i>S</i>
H-15	3.87	3.88	-0.01		3.85	3.88	-0.10	
H-18	3.71	3.72	-0.01	19 <i>R</i>	3.80	3.82	-0.02	19 <i>R</i>

Table 3. ^1H NMR Signals for the Protons of the *threo* and *erythro* Diols¹³ **1** and Acetonide **1b**


	methine proton		acetonide methyl	
	<i>threo</i>	<i>erythro</i>	<i>threo</i>	<i>erythro</i>
diol	3.45 (2H)	3.62, 3.58		
acetonide	3.58 (2H)	4.02, 4.00	1.37 (6H)	1.43, 1.33
1		3.41 (2H)		
1b		3.60 (2H)		1.36 (6H)

of these compounds (see Table 6). Although there have been no reports of any annonaceous acetogenins with this position of the THF ring, it is biogenetically possible to form a THF ring in an odd position from a polyhydroxylated system.

Muricin C (**3**) was isolated as a white waxy solid, $[\alpha]_{\text{D}}^{25} +86.0^\circ$ (c 0.15, CHCl_3). The HRFABMS confirmed the molecular formula of $\text{C}_{35}\text{H}_{65}\text{O}_7$. Successive FABMS fragments at m/z 579, 561, 543, and 525 suggested the presence of four hydroxyl groups, and IR and UV absorptions indicated the presence of an α,β -unsaturated γ -lactone group. Comparisons with the NMR spectral data of **1** suggested that **3** may have the same structural moieties, an α,β -unsaturated γ -lactone with a hydroxyl group at C-4,

**Figure 2.** EIMS fragmentation of muricin A (**1**) and muricin B (**2**).

a mono-THF ring with one flanking hydroxyl group, and a vicinal diol.^{10,11,15}

The placements of the THF ring and hydroxyl groups were established by close examination of the EIMS fragmentation of **3** (see Figure 3). The THF ring was located between C-17/C-20 on the basis of the EIMS peaks at m/z 379 and 309, and the vicinal diol was placed between C-24/C-25 according to the EIMS peaks at m/z ([467]→449→431). Finally, the absolute configuration at C-34 of **3** was determined from its CD spectrum,¹⁴ in which a positive Cotton effect ($\Delta\epsilon > 0$) clearly indicated the *S*-configuration of the C-34 on the γ -lactone fragment. Interestingly, compound **3** is also the first example of an annonaceous acetogenin in which the THF ring begins with another odd position at C-17.

Table 4. ¹H and ¹³C NMR Chemical Shifts of Compounds **3**, **4**, and **5**

	muricin C		muricin D		muricin E	
	δ (¹ H)	δ (¹³ C)	δ (¹ H)	δ (¹³ C)	δ (¹ H)	δ (¹³ C)
1		174.6		174.6		174.6
2		131.2		131.1		131.2
3a	2.52 (m)	32.4	2.50 (m)	32.4	2.50 (m)	32.4
3b	2.40 (m)		2.41 (m)		2.41 (m)	
4	3.86 (m)	70.0	3.82 (m)	69.9	3.84 (m)	69.9
5	1.2–1.5	37.4	1.2–1.5	37.2	1.2–1.5	37.3
6–10	1.2–1.5	25.5–29.9	1.2–1.5	25.5–29.9	1.2–1.5	25.5–29.9
11	1.2–1.5	25.5–29.9	1.2–1.5	25.5–29.9	1.2–1.5	35.4
12	1.2–1.5	25.5–29.9	1.2–1.5	25.5–29.9	3.84 (m)	79.3
13	1.2–1.5	25.5–29.9	1.2–1.5	25.5–29.9	1.99, 1.68 (m)	25.5–29.9
14	1.2–1.5	25.5–29.9	1.2–1.5	35.4	1.99, 1.68 (m)	25.5–29.9
15	1.2–1.5	25.5–29.9	3.82 (m)	79.3	3.84 (m)	81.8
16	1.2–1.5	35.5–35.9	1.99, 1.65 (m)	25.5–29.9	3.41 (m)	74.6 ^a
17	3.86 (m)	79.3	1.99, 1.65 (m)	25.5–29.9	1.2–1.5	33.4–33.7
18	1.97, 1.65 (m)	25.5–29.9	3.82 (m)	81.7	1.2–1.5	25.5–29.9
19	1.97, 1.65 (m)	25.5–29.9	3.43 (m)	74.1 ^a	1.2–1.5	25.5–29.9
20	3.86 (m)	81.7	1.2–1.5	33.3–33.4	1.2–1.5	25.5–29.9
21	3.43 (m)	74.4 ^a	1.2–1.5	33.3–33.4	1.2–1.5	33.4–33.7
22	1.5–1.6	35.5–35.9	3.43 (m)	74.5 ^a	3.41 (m)	74.8 ^a
23	1.2–1.5	35.5–35.9	3.43 (m)	74.2 ^a	3.41 (m)	74.4 ^a
24	3.42 (m)	74.6 ^a	1.2–1.5	33.3–33.4	1.2–1.5	33.4–33.7
25	3.42 (m)	74.3 ^a	1.2–1.5	25.5–29.9	1.2–1.5	25.5–29.9
26	1.2–1.5	31.4–33.5	1.2–1.5	25.5–29.9	1.2–1.5	25.5–29.9
27–28	1.2–1.5	25.5–29.9	1.2–1.5	31.9	1.2–1.5	31.9
29	1.2–1.5	25.5–29.9	1.2–1.5	22.7	1.2–1.5	22.7
30	1.2–1.5	31.4	0.87 (t, <i>J</i> = 6.8)	14.1	0.87 (t, <i>J</i> = 6.8)	14.1
31	1.2–1.5	22.7	7.18 (d, <i>J</i> = 1.2)	151.9	7.18 (d, <i>J</i> = 1.2)	151.9
32	0.88 (t, <i>J</i> = 6.7)	14.1	5.05 (qd, <i>J</i> = 6.8, 1.2)	78.0	5.05 (qd, <i>J</i> = 6.8, 1.2)	78.0
33	7.18 (d, <i>J</i> = 1.2)	151.8	1.42 (d, <i>J</i> = 6.8)	19.1	1.43 (d, <i>J</i> = 6.8)	19.1
34	5.06 (qd, <i>J</i> = 6.8, 1.2)	78.0				
35	1.42 (d, <i>J</i> = 6.8)	19.1				

^a Assignments may be interchangeable.

Muricin D (**4**) was isolated as a white waxy solid, $[\alpha]_{25}^{25}$ _D +77.6° (*c* 0.34, CHCl₃). The molecular formula of C₃₃H₆₁O₇ was determined by HRFABMS. The successive FABMS fragments at *m/z* 551, 533, 515, and 497 suggested the presence of four hydroxyl groups, and IR and UV absorptions indicated the presence of a γ -lactone group. Comparisons with the ¹H and ¹³C NMR spectral data of **1** and **3** suggested that **4** also has the same structural moieties, an α,β -unsaturated γ -lactone with a hydroxyl group at C-4, a mono-THF ring with one flanking hydroxyl group in a conformation of *threo/trans*, and a vicinal diol with a conformation of *threo*, determined according to the methods of Fujimoto et al. (see Table 4).^{10,11,15}

The skeletal structure of the molecule was established by close examination of EIMS fragmentation of **4** (see Figure 4). The fragments at *m/z* 351 and 281 indicated that the THF ring is located between C-15/C-18, and the fragments at *m/z* (439–421) indicated that the diol should be located between C-22/C-23.

Muricin E (**5**) was isolated as a white waxy solid, $[\alpha]_{25}^{25}$ _D +91.4° (*c* 0.23, CHCl₃). The HRFABMS showed a molecular formula of C₃₃H₆₁O₇. Comparisons of FABMS and NMR spectral data with those of **1** and **3** suggested that **5** also possesses the same moieties, an α,β -unsaturated γ -lactone with a hydroxyl group at C-4, a mono-THF ring with one flanking hydroxyl group in a conformation of *threo/trans*, and a vicinal diol with a conformation of *threo*, according to the methods of Fujimoto et al. (see Table 4).^{10,11,15}

The contiguous structure of **5** was established by close examination of the EIMS fragmentation (see Figure 5). The EIMS fragments at *m/z* 309 and 239 demonstrated that the THF ring should be located between C-12/C-15, and the EIMS fragments at *m/z* ([439]→421→403) indicated the diol should be located between C-22/C-23.

Muricin D (**4**) and muricin E (**5**) are the first reported examples of annonaceous acetogenins possessing a C₃₃ skeleton; all other reported annonaceous acetogenins possess a C₃₇ or C₃₅ skeleton.^{1,2}

Muricin F (**6**) was isolated as a white waxy solid, $[\alpha]_{25}^{25}$ _D +48.2° (*c* 0.48, CHCl₃). The molecular formula of C₃₅H₆₃O₇ was established by HRFABMS. The IR, UV, and NMR spectral data revealed that **6** has the same moieties as **1**, an α,β -unsaturated γ -lactone with a hydroxyl group at the C-4 position, a mono-THF ring with one flanking hydroxyl group in a conformation of *threo/trans*, and a vicinal diol with a conformation of *threo* (determined by the methods of Fujimoto et al.; see Table 5).^{10,11,15} Additionally, a proton signal at δ 5.39 (2H), together with the ¹³C NMR signals at δ 130.1 and 129.5, showed the presence of a double bond (see Table 5). The ¹³C NMR chemical shift of the allylic methylene carbon (C-23, δ at 25.5–29.9) suggested the geometry of the double bond as the *Z*-conformation.¹⁶

The structure of **6** was established by close examination of the EIMS fragmentation (see Figure 6). The EIMS peaks at *m/z* 379 and 309 demonstrated that the THF ring is located between C-17/C-20. Furthermore, the location of the double bond at C-24/C-25 was based on EIMS peaks at *m/z* 477 and 423. Finally, the EIMS peak at *m/z* 507 indicated that the diol should be located between C-27/C-28.

Muricin G (**7**), C₃₅H₆₃O₇, was isolated as a white waxy solid, $[\alpha]_{25}^{25}$ _D +47.0° (*c* 0.63, CHCl₃), and its molecular formula was established by HRFABMS. Comparisons of IR, UV, and NMR spectral data with those of **1** and the published data for asiminenin B¹ revealed that **7** is very similar to asiminenin B (see Table 5).

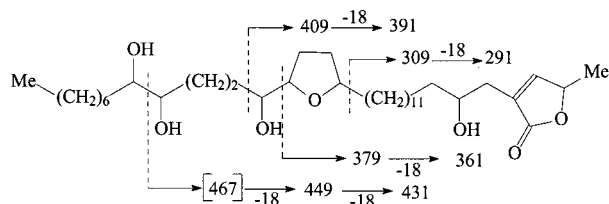
¹H and ¹³C NMR data supported the presence of an α,β -unsaturated γ -lactone with a hydroxyl group at the C-4

Table 5. ^1H and ^{13}C NMR Chemical Shifts of Compounds **6** and **7**

	muricin F		muricin G	
	δ (^1H)	δ (^{13}C)	δ (^1H)	δ (^{13}C)
1		174.6		174.6
2		131.1		131.1
3a	2.52 (m)	32.4	2.50 (m)	33.3–33.4
3b	2.40 (m)		2.41 (m)	
4	3.80 (m)	69.9	3.82 (m)	69.9
5	1.2–1.5	37.4	1.2–1.5	37.3
6–8	1.2–1.5	25.5–29.9	1.2–1.5	25.5–29.9
9	1.2–1.5	25.5–29.9	1.2–1.5	33.3–33.4
10	1.2–1.5	25.5–29.9	3.58	71.7
11	1.2–1.5	25.5–29.9	1.2–1.5	33.3–33.4
12–13	1.2–1.5	25.5–29.9	1.2–1.5	25.5–29.9
14	1.2–1.5	25.5–29.9	1.2–1.5	37.2
15	1.2–1.5	25.5–29.9	3.43 (m)	74.0
16	1.2–1.5	33.1–35.4	3.89 (m)	82.6 ^a
17	3.86 (m)	79.3	1.99, 1.65 (m)	25.5–29.9
18	1.97, 1.65 (m)	25.5–29.9	1.99, 1.65 (m)	25.5–29.9
19	1.97, 1.65 (m)	25.5–29.9	3.89 (m)	82.6 ^a
20	3.86 (m)	81.7	3.43 (m)	73.5
21	3.43 (m)	74.4 ^a	1.2–1.5	33.3–33.4
22	1.5–1.6	33.1–35.4	2.17 (m)	25.5–29.9
23	2.01	25.5–29.9	5.36 (m)	130.8
24	5.39 (m)	130.1	5.36 (m)	128.9
25	5.39 (m)	129.5	2.17 (m)	25.5–29.9
26	2.01	33.1–35.4	1.2–1.5	25.5–29.9
27	3.42 (m)	74.6 ^a	1.2–1.5	25.5–29.9
28	3.42 (m)	74.3 ^a	1.2–1.5	25.5–29.9
29	1.2–1.5	33.1–35.4	1.2–1.5	25.5–29.9
30	1.2–1.5	31.4	1.2–1.5	31.9
31	1.2–1.5	22.6	1.2–1.5	22.7
32	0.87 (t, $J = 6.7$)	14.0	0.87 (t, $J = 6.8$)	14.1
33	7.18 (d, $J = 1.2$)	151.9	7.18 (d, $J = 1.2$)	151.9
34	5.06 (qd, $J = 6.8, 1.2$)	78.0	5.05 (qd, $J = 6.8, 1.2$)	78.0
35	1.42 (d, $J = 6.8$)	19.1	1.41 (d, $J = 6.8$)	19.1

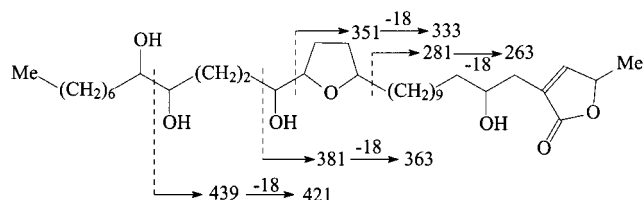
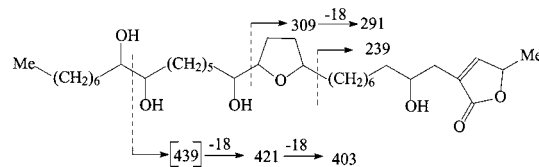
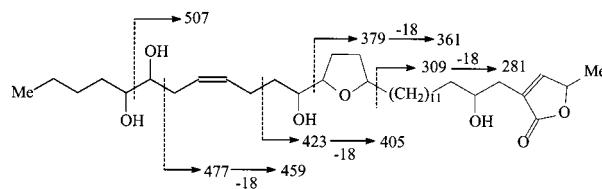
^a Assignments may be interchangeable.**Table 6.** Cytotoxic IC_{50} Values of Compounds **1–12** against Human Hepatoma Cell Lines

treatment	human hepatoma cell lines	
	Hep G ₂ IC_{50} ($\mu\text{g/mL}$)	Hep 2,2,15 IC_{50} ($\mu\text{g/mL}$)
muricin A (1)	5.04	5.13×10^{-3}
muricin B (2)	1.78	4.29×10^{-3}
muricin C (3)	4.99×10^{-1}	3.87×10^{-3}
muricin D (4)	6.60×10^{-4}	4.80×10^{-2}
muricin E (5)	NT ^a	NT
muricin F (6)	4.28×10^{-2}	3.86×10^{-3}
muricin G (7)	NT	NT
muricatetrocins A&B (8, 9)	4.95×10^{-2}	4.83×10^{-3}
longifolicin (10)	4.04×10^{-4}	4.90×10^{-3}
corossolin (11)	3.53×10^{-1}	2.34×10^{-1}
corossolone (12)	4.80×10^{-1}	2.84×10^{-1}
adriamycin	2.41×10^{-1}	4.50×10^{-1}

^a NT = not tested.**Figure 3.** EIMS fragmentation of muricin C (**3**).

position and a mono-THF ring with two flanking hydroxyl groups in the conformation of *threo/trans/threo*.^{10,11,15}

The structure of **7** was further established by close examination of EIMS fragmentation (see Figure 7). The EIMS fragment at m/z 241 (cleavage between C-11/C-10)

**Figure 4.** EIMS fragmentation of muricin D (**4**).**Figure 5.** EIMS fragmentation of muricin E (**5**).**Figure 6.** EIMS fragmentation of muricin F (**6**).

and its daughter peak at m/z 223 (cleavage between C-11/C-10 – H_2O) suggested that the final hydroxyl group should be located at C-10. The EIMS peaks at m/z 397 and 309 demonstrated the location of the THF ring should be between C-16/C-19. Finally, the peak at m/z 495 suggested that the double bond should be located at C-23/C-24. The ^{13}C NMR chemical shifts of the allylic methylene carbons

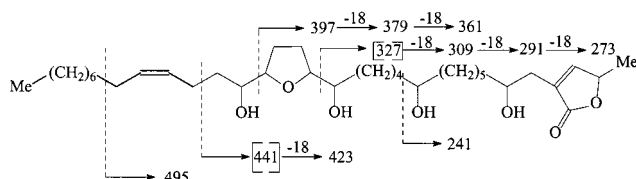


Figure 7. EIMS fragmentation of muricin G (7).

(C-22 and C-25, δ at 25.5–29.9) suggested the geometry of the double bond as the *Z*-conformation.¹⁶

All the CD spectra of compounds 4–7 showed a positive π - π^* Cotton effect ($\Delta\epsilon > 0$), indicating the *S*-configuration of C-34 on the γ -lactone fragment, as is the case for compounds 1, 2, and 3.

The identities of the five known acetogenins were verified by comparing UV, IR, ¹H and ¹³C NMR, and MS data with published values to identify a mixture of muricatetrocin A (8) and muricatetrocin B (9),⁵ longifolicin (10),⁶ corossolin (11),⁷ and corossolone (12).⁷

In conclusion, seven new annonaceous acetogenins, as well as five known ones, were identified from the seeds of *Annona muricata* and confirmed on the basis of spectral analyses. The odd initial position of the THF ring (compounds 1–3 and 6) and the shorter aliphatic chain (compounds 4 and 5) are new and unusual structural features of the annonaceous acetogenins.

Bioactivities and SAR. Compounds 1–12 except for compounds 5 and 7 were tested against the human hepatoma cancer cell lines Hep G₂ and 2,2,15.^{17,18} The results are summarized in Table 6. Following the strategy of Miyoshi et al.,¹⁹ the structure–activity relationships of the tested compounds are discussed below by consideration of four chemical portions: the hydroxylated THF ring moiety, the α,β -unsaturated γ -lactone ring moiety, the spacer moiety linking the two rings, and the alkyl side chain attached to the THF rings, which often has a diol group and ends with the terminal methyl.

The Role of the Stereochemistry of the Hydroxyl Group at C-4. Compounds 1 and 2, in which the only difference is the orientation of the hydroxyl group at C-4, had similar bioactivities, although they were less potent than adriamycin against Hep G₂. However, compound 1, with the *R*-hydroxyl group at C-4, is 2.5 times more potent than compound 2, which is the *S*-form. Miyoshi et al.¹⁸ suggest that the presence of the 4-OH group in the spacer region is not essential for activity; however, the stereochemical difference of the 4-OH of 1 and 2 appears to be the only reason for the different bioactivities.

The Role of the Spacer Moiety Linking the Two Rings. In comparing the cytotoxic values (IC₅₀) of compounds 3 and 4 against the Hep 2,2,15 cell line, it appears that the shorter length of the spacer moiety is associated with weaker potency; however, this was not the case against Hep G₂. Comparison with compounds 8 and 9 suggested that the appropriate length, approximately 12 carbons (from C-3 to C-14), should be more potent against Hep G₂.

The Role of Hydroxyl Groups in the Alkyl Side Chain. Against Hep G₂, comparisons with compounds 1, 2, and 4 indicated that increasing the length between the THF ring and the diol group leads to weaker potency.

The Role of the Double Bond in the Alkyl Side Chain. Of the annonaceous acetogenins containing a mono-THF ring with one flanking hydroxyl group (3 and 6), compound 6 was the most cytotoxic against both Hep G₂ and 2,2,15, suggesting that the presence of the double bond may enhance the bioactivity.

Summarizing the observation regarding structure and bioactivity, the spacer moiety of annonaceous acetogenins is very important for maximizing their potency. Moreover, the above bioassay data imply that there are maximal features in finding an agent more selective against Hep G₂ and 2,2,15.

Experimental Section

General Experimental Procedures. Optical rotations were measured with a JASCO DIP-370 digital polarimeter. The IR spectra were measured on a Hitachi 260-30 spectrophotometer. ¹H NMR (400 MHz) and ¹³C NMR (100 MHz) spectra (all in CDCl₃) were recorded with Varian NMR spectrometers, using TMS as internal standard. LRFABMS and LREIMS were obtained with a JEOL JMS-SX/SX 102A mass spectrometer or a Quattro GC/MS spectrometer having a direct inlet system. HRFABMS were measured on a JEOL JMS-HX 110 mass spectrometer. CD was measured on a JASCO DIP 370 polarimeter. Si gel 60 (Macherey-Nagel, 230–400 mesh) was used for column chromatography; precoated Si gel plates (Macherey-Nagel, SIL G-25 UV₂₅₄, 0.25 mm) were used for analytical TLC, and precoated Si gel plates (Macherey-Nagel, SIL G/UV₂₅₄, 0.25 mm) were used for preparative TLC. The spots were detected by Dragendorff's reagent, Kedde's reagent,²⁰ or 50% H₂SO₄ and then heating on a hot plate. HPLC was performed on a JASCO PU-980 apparatus equipped with an UV-970 detector. Develosil ODS-5 (250 × 4.6 mm i.d.) and preparative ODS-5 (250 × 20 mm i.d.) columns were used for analytical and preparative purposes, respectively.

Plant Material. The seeds of *A. muricata* were collected from Chia-Yi City, Taiwan, in March 1997. A voucher specimen is deposited in the Graduate Institute of Natural Products, Kaohsiung, Taiwan, Republic of China.

Extraction and Isolation. The seeds (1.0 kg) were extracted repeatedly with MeOH at room temperature. The combined MeOH extracts were evaporated and partitioned to yield CHCl₃ and aqueous extracts. The CHCl₃ layer afforded a waxy extract (ca. 200.6 g), positive to Kedde's reagent. It was further separated into 10 fractions by column chromatography on Si gel with gradient systems of *n*-hexane–CHCl₃ (*n*-hexane–CHCl₃, 4:1, to pure CHCl₃) and CHCl₃–MeOH (pure CHCl₃ to CHCl₃–MeOH, 10:1). Longifolicin (10),⁶ corossolin (11),⁷ and corossolone (12)⁷ were further purified from fraction 8 by reversed-phase HPLC (Hypersil ODS-5 column, 250 × 5 mm, MeOH–water, 97:3, flow rate of 1 mL/min; UV detector set at 225 nm). The remnant of fraction 8 was then combined with fraction 9 and further separated into 10 fractions with the solvent system of *n*-hexanes–EtOAc, 1:1, by column chromatography. Muricin A (1), muricin B (2), muricin C (3), and muricin F (6) were isolated and purified from the seventh fraction by preparative reversed-phase HPLC (ODS-5 column) with 88:12 MeOH–water (flow rate of 2 mL/min; UV detector set at 225 nm). Muricin D (4), muricin E (5), and muricin G (7), as well as two known compounds, muricatetrocin A (8) and muricatetrocin B (9),⁵ were isolated and purified from the eighth fraction by preparative reversed-phase HPLC (ODS-5 column) with 86:14 MeOH–water (flow rate of 2 mL/min; UV detector set at 225 nm).

Muricin A (1): white waxy solid; [α]_D²⁵ +7.2° (c 0.25, CHCl₃); UV (MeOH) λ_{\max} (log ϵ) 210 (3.64) nm; IR (KBr) ν_{\max} 3392 (OH), 2917, 2849, 1746 (OC=O), 1067 cm⁻¹; ¹H NMR (CDCl₃, 400 MHz) and ¹³C NMR (CDCl₃, 100 MHz) data, see Table 1; FABMS *m/z* 597 [MH]⁺; EIMS (30 eV) 381 (2), 363 (1), 351 (11), 333 (11), 281 (30), 263 (2), 239 (19), and 221 (5), see Figure 2; HRFABMS *m/z* 597.4726 (calcd for C₃₅H₆₄O₇, 597.4730).

Muricin B (2): white waxy solid; [α]_D²⁵ 0° (c 0.11, CHCl₃); UV (MeOH) λ_{\max} (log ϵ) 210 (3.65) nm; IR (KBr) ν_{\max} 3419 (OH), 2918, 2849, 1738 (OC=O), 1067 cm⁻¹; ¹H NMR (CDCl₃, 400 MHz) and ¹³C NMR (CDCl₃, 100 MHz) data, see Table 1; FABMS *m/z* 597 [MH]⁺; EIMS (30 eV) 381 (2), 363 (1), 351 (10), 333 (11), 281 (30), 263 (2), 239 (19), and 221 (5), see Figure 2; HRFABMS *m/z* 597.4731 (calcd for C₃₅H₆₄O₇, 597.4730).

(R)- and (S)-MTPA Derivatives of 1 and 2. Compounds **1** (5 mg) and **2** (5 mg) were dissolved in 1 mL of dry CH₂Cl₂, 0.5 mL of pyridine, and 1 mg of 4-(dimethylamino)pyridine, and 100 mg of (R)-(-)-methoxyl- α -(trifluoromethyl)phenylacetyl chloride was introduced to the solution. After the reaction mixture was allowed to sit for more than 6 h at room temperature (the reaction progress was monitored by TLC), saturated NaHCO₃ (~3 mL) and Et₂O (~3 mL) were added. The organic phase was removed, and the aqueous phase was extracted with Et₂O (~5 mL, 2 \times). The organic phases were combined, washed three times with NaHSO₄ (5% aqueous solution, to remove pyridine) and brine, dried (MgSO₄), and concentrated under reduced pressure to leave a crude yellow oil,²⁰ which was purified by preparative TLC to give the (S)-MTPA esters. The (R)-MTPA esters were prepared in the same way using (S)-(+)-methoxyl- α -(trifluoromethyl)phenylacetyl chloride reagent.

Acetonide Derivative of 1. Compound **1** (2 mg) and 0.1 mg of toluenesulfonic acid monohydrate were dissolved in 0.5 mL of acetone. The mixture was allowed to stand at room temperature for 5 h, and the conversion was monitored by TLC. The product was purified over a small column of Si gel (in a small pipet) eluted with 20:1 hexane–acetone and was dried in vacuo to give the acetonide derivative **1b**.

Muricin C (3): white waxy solid; [α]²⁵_D +86.0° (*c* 0.15, CHCl₃); UV (MeOH) λ_{\max} (log ϵ) 208 (3.73) nm; IR (KBr) ν_{\max} 3440 (OH), 2930, 2833, 1745 (OC=O), 1027 cm⁻¹; ¹H NMR (CDCl₃, 400 MHz) and ¹³C NMR (CDCl₃, 100 MHz) data, see Table 3; FABMS *m/z* 597 [MH]⁺; EIMS (30 eV) 449 (1), 431 (1), 409 (1), 391 (1), 379 (6), 361 (9), 309 (16), 291 (3), 267 (10), and 239 (5), see Figure 3; HRFABMS *m/z* 597.4732 (calcd for C₃₅H₆₄O₇, 597.4730).

Muricin D (4): white waxy solid; [α]²⁵_D +77.6° (*c* 0.34, CHCl₃); UV (MeOH) λ_{\max} (log ϵ) 208 (3.69) nm; IR (KBr) ν_{\max} 3432 (OH), 2925, 2854, 1745 (OC=O), 1462, 1319, 1082 cm⁻¹; ¹H NMR (CDCl₃, 400 MHz) and ¹³C NMR (CDCl₃, 100 MHz) data, see Table 3; FABMS *m/z* 569 [MH]⁺; EIMS (30 eV) 439 (1), 421 (1), 403 (1), 381 (2), 363 (1), 351 (30), 333 (21), 281 (64), 263 (4), 239 (40), and 221 (7), see Figure 4; HRFABMS *m/z* 569.4416 (calcd for C₃₃H₆₀O₇, 569.4417).

Muricin E (5): white waxy solid; [α]²⁵_D +91.4° (*c* 0.23, CHCl₃); UV (MeOH) λ_{\max} (log ϵ) 208 (3.62) nm; IR (KBr) ν_{\max} 3334 (OH), 2916, 2847, 1733 (OC=O), 1082 cm⁻¹; ¹H NMR (CDCl₃, 400 MHz) and ¹³C NMR (CDCl₃, 100 MHz) data, see Table 3; FABMS *m/z* 569 [MH]⁺; EIMS (30 eV) 421 (1), 403 (1), 351(7), 333 (10), 309 (4), 291 (2), 263 (4), and 239 (24), see Figure 5; HRFABMS *m/z* 569.4417 (calcd for C₃₃H₆₀O₇, 569.4417).

Muricin F (6): white waxy solid; [α]²⁵_D +48.2° (*c* 0.48, CHCl₃); UV (MeOH) λ_{\max} (log ϵ) 208 (3.89) nm; IR (KBr) ν_{\max} 3407 (OH), 2925, 2854, 1743 (OC=O), 1078 cm⁻¹; ¹H NMR (CDCl₃, 400 MHz) and ¹³C NMR (CDCl₃, 100 MHz) data, see Table 5; FABMS *m/z* 595 [MH]⁺; EIMS (30 eV) 507 (1), 477 (1), 459 (1), 423 (1), 405 (1), 379 (2), 361 (2), 309 (7), 281 (15), 263 (3), 239 (12), and 109 (13), see Figure 6; HRFABMS *m/z* 595.4573 (calcd for C₃₅H₆₂O₇, 595.4574).

Muricin G (7): white waxy solid; [α]²⁵_D +47.0° (*c* 0.63, CHCl₃); UV (MeOH) λ_{\max} (log ϵ) 210 (3.52) nm; IR (KBr) ν_{\max} 3386 (OH), 2931, 2859, 1748 (OC=O), 1081 cm⁻¹; ¹H NMR (CDCl₃, 400 MHz) and ¹³C NMR (CDCl₃, 100 MHz) data, see Table 5; FABMS *m/z* 595 [MH]⁺; EIMS (30 eV) 495 (1), 423 (1), 397 (1), 379 (2), 361 (6), 309 (44), 291 (15), 273 (7), and 241 (13), see Figure 7; HRFABMS *m/z* 595.4574 (calcd for C₃₅H₆₂O₇, 595.4574).

A Mixture of Muricatetrocin A (8) and Muricatetrocin B (9): colorless oil; [α]²⁵_D +22.2° (*c* 0.25, CHCl₃); UV (MeOH) λ_{\max} (log ϵ) 210 (3.94) nm; UV, MS, and ¹H and ¹³C NMR data were identical with published values.⁵

Longifolicin (10): colorless oil; [α]²⁵_D +8.3° (*c* 0.12, CHCl₃); UV (MeOH) λ_{\max} (log ϵ) 208 (3.98) nm; UV, MS, and ¹H and ¹³C NMR data were identical with published values.⁶

Corosolin (11): waxy solid; [α]²⁵_D +82.8° (*c* 0.34, CHCl₃); UV (MeOH) λ_{\max} (log ϵ) 210 (3.78) nm; UV, MS, and ¹H and ¹³C NMR data were identical with published values.⁷

Corosolone (12): waxy solid; [α]²⁵_D +11.7° (*c* 0.19, CHCl₃); UV (MeOH) λ_{\max} (log ϵ) 206 (3.98) nm; UV, MS, and ¹H and ¹³C NMR data were identical with published values.⁷

Bioassays. Human hepatoma cell (Hep G2) and Hep G2 cell transfected with HBV (Hep 2,2,15) were cultured in RPMI 1640 and DMEM medium containing 10% FCS, 100 units/mL penicillin, and 100 μ g/mL streptomycin. All the cell lines were maintained in an incubator at 37 °C in humidified air containing 5% CO₂. The activity against various cancer cells was determined by the methylene blue colorimetric method as previously reported.^{10,17,18} The plates were read immediately on an enzyme-linked immunosorbent microplate reader (ELISA Biokinetics Reader) at a wavelength of 592 nm. The 50% inhibition concentration (IC₅₀) was defined as 50% reduction of absorbance in the control assay without drugs.^{10,17,18}

Acknowledgment. The investigation was supported by a grant from the National Health Research Institute of the Republic of China awarded to Y.C.W. (NHRI-GT-EX89B806P).

References and Notes

- Zeng, L.; Ye, Q.; Oberlies, N. H.; Shi, G.; Gu, Z. M.; He, K.; McLaughlin J. L. *Nat. Prod. Rep.* **1996**, *13*, 275–306.
- Zafra-Polo, M. C.; Figadère, B.; Gallardo, T.; Tormo, J. R.; Cortes, D. *Phytochemistry* **1998**, *48*, 1087–1117.
- Alali, F. Q.; Liu, X. X.; McLaughlin, J. L. *J. Nat. Prod.* **1999**, *62*, 504–540.
- Li, C. M.; Mu, Q.; Hao, X. J.; Sun, H. D.; Zheng, H. L.; Wu, Y. C. *Chin. Chem. Lett.* **1994**, *5*, 747–750.
- Rieser, M. J.; Fang, X. P.; Anderson, J. E.; Miesbauer, L. R.; Smith, D. L.; McLaughlin, J. L. *Helv. Chim. Acta* **1993**, *76*, 2433–2443.
- Ye, Q.; Alfonso, D.; Evert, D.; McLaughlin, J. L. *Bioorg. Med. Chem.* **1996**, *4*, 537–545.
- Cortes, D.; Myint, S. H.; Laurens, A.; Hocquemiller, R.; Leboeuf, M.; Cavé, A. *Can. J. Chem.* **1991**, *69*, 8–11.
- Rieser, M. J.; Hui, Y. H.; Rupperecht, J. K.; Kozłowski, J. F.; Wood, K. V.; McLaughlin, J. L.; Hanson, P. R.; Zhuang, Z.; Hoye, T. R. *J. Am. Chem. Soc.* **1992**, *114*, 10203–10213.
- Liaw, C. C.; Chang, F. R.; Chen, Y. Y.; Chiu, H. F.; Wu, M. J.; Wu, Y. C. *J. Nat. Prod.* **1999**, *63*, 1613–1617.
- Chang, F. R.; Chen, J. L.; Lin, C. Y.; Chiu, H. F.; Wu, M. J.; Wu, Y. C. *Phytochemistry* **1999**, *51*, 883–889.
- Chen, Y. C.; Chang, F. R.; Chiu, H. F.; Wu, M. J.; Wu, Y. C. *Phytochemistry* **1999**, *51*, 429–433.
- Hoye, T. R.; Hanson, P. R.; Hasenwinkel, L. E.; Ramirez, E. A.; Zhuang, Z. *Tetrahedron Lett.* **1994**, *35*, 8529–8532.
- Chávez, D.; Mata, R. *J. Nat. Prod.* **1998**, *61*, 580–584.
- Gawronski, J.; Wu, Y. C. *Polish J. Chem.* **1999**, *73*, 241–243.
- Fujimoto, Y.; Murasaki, C.; Shimada, H.; Nishioka, S.; Kakinuma, K.; Singh, S.; Gupta, Y. K.; Sahai, M. *Chem. Pharm. Bull.* **1994**, *42*, 1175–1184.
- Dorman, D. E.; Jautelat, M.; Roberts, J. D. *J. Org. Chem.* **1971**, *36*, 2757–2766.
- Doong, S. L.; Tsai, C. H.; Schinazi, R. F.; Liotta, D. C.; Cheng, Y. C. *Proc. Natl. Acad. Sci., U.S.A.* **1991**, *88*, 8495–8499.
- Elliott, W. M.; Auersperg, N. *Biotech. Histochem.* **1993**, *68*, 29–35.
- Miyoshi, H.; Ohshima, M.; Shimada, H.; Akagi T.; Iwamura, H.; McLaughlin, J. L. *Biochim. Biophys. Acta* **1998**, *1365*, 443–452.
- Hsu, Z. S. *Natural Product Chemistry*; Sciences Press: Beijing, 1993; Chapter 11, p 497 (ISBN 7-03-002506-7).

NP010035S